

PAPER

Enhancing the efficiency of low bandgap conducting polymer bulk heterojunction solar cells using P3HT as a morphology control agent

Cite this: *J. Mater. Chem. A*, 2013, **1**, 2447

Sheng-Yung Chang,^a Hsueh-Chung Liao,^b Yu-Tsun Shao,^c Yu-Ming Sung,^c Sheng-Hao Hsu,^d Chun-Chih Ho,^b Wei-Fang Su^{*b} and Yang-Fang Chen^{*c}

The development of low bandgap conducting polymers has made bulk heterojunction solar cells a viable low cost renewable energy source. The high boiling point of 1,8-diiodooctane (DIO) is usually used to control the morphology of the active layer consisting of a conducting polymer and PCBM, so that a high power conversion solar cell can be achieved. We report here an alternative approach using nonvolatile, crystalline and conducting P3HT as an effective morphology control agent. A model system of PCPDTBT/PC61BM was selected for this study. The change of optoelectronic properties with the introduction of P3HT was monitored by measuring the absorption spectra and charge carrier mobility, and the morphology change with the introduction of P3HT in the active layer was monitored by AFM, TEM, and GIXRD. The results indicate that favorable bi-continuous phase separation and appropriate domain size of each phase can be achieved to facilitate fast charge transport, and thus improve the power conversion efficiency of the solar cell. By adding 1 wt% P3HT into the blend of PCPDTBT/PC61BM, the power conversion efficiency can be improved by 20%. Moreover, with the incorporation of 1 wt% P3HT to the blend of PCPDTBT/PC61BM with DIO, the power conversion efficiency can be further increased by 17%. The strategy of this study can be expanded to other low bandgap conducting polymers for high efficiency bulk heterojunction solar cells.

Received 5th November 2012
Accepted 10th December 2012

DOI: 10.1039/c2ta00990k

www.rsc.org/MaterialsA

Introduction

The organic photovoltaic cell (OPV) is a low cost candidate to resolve the impending energy shortage in the near future.¹ For a high efficiency OPV, a bulk heterojunction (BHJ) of an active layer made from a blend of a conducting polymer and a fullerene derivative is usually needed. As compared with the commonly used poly(3-hexylthiophene), low bandgap polymers can improve the cell efficiency by extending the light harvesting to the near infrared (NIR) solar spectrum from 1.4 to 1.9 eV, and increasing open circuit voltage (V_{oc}).^{2–6} Poly[2,1,3-benzothiadiazole-4,7-diyl[4,4-bis(2-ethylhexyl)-4*H*-cyclopenta[2,1-*b*;3,4-*b'*]-dithiophene)-2,6-diyl] (PCPDTBT) is known to be an efficient low bandgap polymer, which will be used and blended with [6,6]-phenyl-C61-butyric acid methyl ester (PC61BM) as our model system to achieve a highly efficient organic solar cell. A

low bandgap polymer usually consists of alternating donor and acceptor building blocks in the polymer chain, which makes it difficult to form a highly crystalline structure and ideal bicontinuous paths with fullerene for efficient charge transport. Several methods have been developed to obviate this morphological problem. For example, applying a thermal annealing process can improve the polymer crystalline phase in the blend.^{7,8} However this approach is not good for the blend of the low bandgap polymer and fullerene, and even leads to negative effects.⁹ Adding a solvent-type additive to tune the morphology of the BHJ is an alternative way to improve the cell performance. For the device made from the PCPDTBT/PC71BM blend, incorporating a few volume percentage of 1,8-diiodooctane (DIO) into the solvent allows the film morphology to be well-engineered. The power conversion efficiency is also enhanced due to the formation of interpenetrating channel-like domains and well-separated electron donor and acceptor phases.^{5,10} These morphological features are indispensable for producing high efficiency BHJ solar cells.^{11–15} The idea of ternary blend solar cells is also a good approach to achieve high performance OPV devices by incorporating “complementary” material. A successful study on this topic incorporated PCPDTBT into the blend of poly(3-hexylthiophene) (P3HT) and PC61BM system to extend the absorption spectrum of the device. The PCPDTBT can help to harvest more photons for P3HT/PC61BM in order to

^aGraduate Institute of Applied Physics, National Taiwan University, No. 1, Sec. 4, Roosevelt Road, Taipei 106-17, Taiwan

^bDepartment of Materials Science and Engineering, National Taiwan University, Taipei 106-17 No. 1, Sec. 4, Roosevelt Road, Taiwan. E-mail: suwf@ntu.edu.tw; Fax: +886 2 33664078; Tel: +886 2 33664078

^cDepartment of Physics, National Taiwan University, No. 1, Sec. 4, Roosevelt Road, Taipei 106-17, Taiwan. E-mail: yfchen@phys.ntu.edu.tw; Tel: +886 2 33665125

^dInstitute of Polymer Science and Engineering, National Taiwan University, No. 1, Sec. 4, Roosevelt Road, Taipei 106-17, Taiwan

compensate for the scarce utilization of photons in the NIR region.¹⁶ A similar concept of adding high-absorption small molecules to the binary blend bi-layered and BHJ system has also been demonstrated.¹⁷ In addition, mixing two kinds of polymers (*e.g.* a polymer blend) with fullerene to produce a ternary device has been studied.^{18–21} However, the polymer blend often leads to severe phase separation and results in micrometer domain sizes. By adding a small amount of an alternating copolymer of PCPDTBT into the P3HT/PC61BM system, the severe phase separation was not observed.¹⁶ Previous studies have suggested that by adding an equal weight ratio,²² or more than 5 wt%,¹⁷ of P3HT to PCPDTBT/PC61BM, the amorphous phase present in the BHJ leads to poor charge transport.

Thus, we postulated that using less than 5 wt% crystalline P3HT in PCPDTBT/PC61BM as a morphology control agent should induce crystallization in this ternary system with the desired bi-continuous domain size for efficient charge separation and high cell performance. The crystalline P3HT agent also exhibits additional advantages over DIO which can compensate for the short wavelength absorption in the system.

Experimental details

PCPDTBT (1-Material, Quebec, Canada, 99.99%), PC61BM (Nano-C, Inc. USA, 99.5%), 1,8-diiiodooctane (DIO) (Alfar Aesar, USA, 98%) and PEDOT/PSS (Baytron 4083) were purchased. Regioregular high molecular weight P3HT ($M_w \approx 62$ kDa, PDI < 1.5, RR > 95%) was synthesized following the procedure demonstrated previously.²³ The blend solutions were composed of 10 mg PCPDTBT, 36 mg PC61BM, and different amounts of P3HT (*i.e.* 0.5 mg, 1 mg, or 2 mg). The resulting concentrations of P3HT in the solution were 1%, 2%, and 4% by weight ratio, respectively. Subsequently, the mixtures were dissolved in 1 ml chlorobenzene, or 0.997 ml chlorobenzene and 0.003 ml DIO (3 vol%), and then stirred at 70 °C for 2 days. The control set of PCPDTBT/PC61BM blend solutions were also prepared by mixing 10 mg PCPDTBT and 36 mg PC61BM in chlorobenzene or chlorobenzene + 3 vol% DIO. In our layer-by-layer organic photovoltaic device fabrication, all of the solutions were processed in air. The transparent electrode ITO glass (Merck) was ultrasonically cleaned with ammonia/H₂O₂/ultra-pure water, methanol, and isopropyl alcohol in sequence, and then treated with oxygen plasma. A thin hole transport layer (40–60 nm) of PEDOT/PSS was spin-coated onto the cleaned ITO substrate and then baked at 120 °C for 15 min. After cooling, the active layer was spin coated at 2500 rpm for 1 min using the blend solution. The typical active layer thickness varied from 100 to 130 nm. Finally, the upper cathode calcium (~45 nm) and aluminum (~100 nm) were thermally evaporated under high vacuum conditions ($<5 \times 10^{-6}$ Torr) in sequence. The typical device had a working area of 0.063 cm².

The devices were characterized using a New Port Inc. type 69920 at AM 1.5, 100 MW cm⁻² under air, and their external quantum efficiencies (EQE) were measured using a set up made from a New Port Inc. type 69911 and an ENLI Tech. QE R3015.

The absorption properties of the active layer were measured with a Perkin Elmer Inc. Lambda 35. To obtain the charge carrier mobility of the active layer, an electron-only device was fabricated by spin-coating the active layer film onto a glass substrate which was sandwiched between two Al electrodes (about 100 nm each), and a hole-only device was manufactured by spin-coating the active layer onto an ITO substrate, and then thermally evaporating a 100 nm Ag electrode onto it. We used the space charge limited current (SCLC) model to determine the charge carrier mobility of the active layer using the following formula:^{31–33}

$$J = \frac{9 \epsilon \epsilon_0 \mu}{8 L^3} V_{\text{eff}}^2 \exp\left(0.89 \sqrt{\frac{V}{E_0 L}}\right) \quad (1)$$

The active layer film was spin-coated onto a pre-cleaned 1 cm × 1 cm silicon wafer for atomic force microscopy (AFM) measurements using a Digital Instruments Inc. Dimension-3100 Multimode scope. For transmission electron microscopy (TEM) observations, the active layer samples were microtomed into 100 nm slices and then the TEM images were taken with a JEOL 1230 microscope operated at an accelerating voltage of 100 kV. The grazing incidence X-ray diffraction (GIXRD) measurement was launched at the BL17A endstation of the National Synchrotron Radiation Research Center of Taiwan. The instrumental setup of the GIXRD followed the report in the literature.²⁴ With a monochromated X-ray beam (9 keV, wavelength = 1.33 Å, incidence angle = 0.2°), the 3450 × 3450 pixel resolution GIXRD scans were simultaneously collected by a Mar345 Imaging Plate Area Detector, Fuji Bas 2500 IP, Bircrondetector, and then addressed and transferred by the relevant software of the Mar345 Control Software, Fit2D, WinPlotr, GSAS, Spec. The effective Q range of GIXRD is from 0.2 to 3 Å⁻¹. The 1D profiles were obtained by integrating the 2D patterns along Q_z for out-of-plane directions.

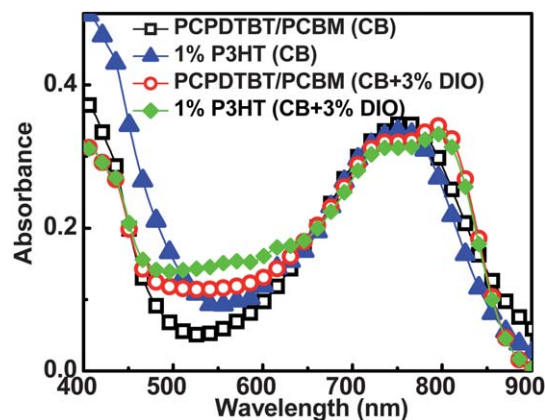


Fig. 1 Absorption spectra of PCPDTBT/PC61BM (wt ratio = 10 : 36, black square), PCPDTBT/PC61BM with 1 wt% P3HT (wt ratio = 10 : 36 : 0.5, blue triangle) thin films processed by chlorobenzene solvent (CB). The other sets of data are PCPDTBT/PC61BM (wt ratio = 10 : 36, red circle) and PCPDTBT/PC61BM with 1 wt% P3HT (wt ratio = 10 : 36 : 0.5, green diamond) thin films processed with CB + 3 vol% DIO.

Results and discussion

Fig. 1 shows the UV-vis absorption spectra of the PCPDTBT/PC61BM/P3HT blend films. The λ_{max} of 750 nm is the characteristic absorption of PCPDTBT. The new peak at 800 nm is due to the aggregation of the π -conjugated polymer of PCPDTBT.^{5,26–29} The presence of 1 wt% P3HT in PCPDTBT/PC61BM or PCPDTBT/PC61BM/DIO causes a significant absorption enhancement from 450 to 650 nm, due to the main chain absorption of P3HT and intermolecular π - π stacking of P3HT.³⁰ Therefore, the photocurrent of the device is expected to increase.¹⁶

The electron mobility and hole mobility of the active layer were determined by the SCLC model^{31–33} as shown in Fig. 2(a) and (b), respectively, and are summarized in Table 1. The electron mobility of a conducting polymer is usually lower than its hole mobility by an order of magnitude ($\mu_e/\mu_h = 0.15$). The addition of DIO in PCPDTBT/PC61BM can increase the electron mobility (Fig. 2a) by an order of magnitude, but hole mobility is not increased that much (Fig. 2b). When 1 wt% P3HT is incorporated into the active layer, its electron mobility is noticeably enhanced, regardless of whether the layer contains DIO or not. Thus, a more balanced charge transport ($\mu_e/\mu_h = 0.18$ for the system without DIO, 1.63 with DIO) was obtained in the thin

Table 1 The electron and hole mobilities obtained from the SCLC measurements of PCPDTBT/PC61BM and PCPDTBT/PC61BM/P3HT blend films

Thin film	μ_e ($\text{cm}^2 \text{V s}^{-1}$)	μ_h ($\text{cm}^2 \text{V s}^{-1}$)
PCPDTBT/PC61BM (CB)	1.7×10^{-6}	1.1×10^{-5}
1% P3HT (CB)	3.4×10^{-6}	1.9×10^{-5}
PCPDTBT/PC61BM (CB + 3% DIO)	3.3×10^{-5}	1.7×10^{-5}
1% P3HT (CB + 3% DIO)	5.9×10^{-5}	3.6×10^{-5}

film of ternary blend PCPDTBT/PC61BM/P3HT due to the enhanced hole and electron mobility. We can deduce from this result that appropriate charge carrier pathways are formed among the donor and acceptor materials by the incorporation of P3HT into the blend.

The J - V curves, V_{oc} , J_{sc} and power conversion efficiencies (PCEs) of the devices fabricated from the ternary blend of PCPDTBT/PC61BM/P3HT (1 wt%) are shown in Fig. 3 and Table 2. The table also contains the data for the devices fabricated with a higher wt% of P3HT. A significant improvement of performance of 1.3 times was observed when 1 wt% of P3HT was added to PCPDTBT/PC61BM. However, the improved performance decreased when the amount of P3HT added was higher than 1 wt%. This could be attributed to deteriorated phase separation, which was caused by the excess amount of the second polymer.¹⁷ When the solvent for the processing of the active layer contained 3 vol% DIO, the PCE of the device was raised substantially by increasing J_{sc} and FF while decreasing V_{oc} . This observation may be due to the lowering of the energy of the charge transfer states.²⁹ In the system of PCPDTBT/PC61BM/DIO, the addition of 1 wt% P3HT improved the PCE of the cell by 1.2 times from 2.9 to 3.4%, due to the improvement of J_{sc} and FF.

We further investigated the contribution of adding P3HT to the active layer for improved cell performance by external

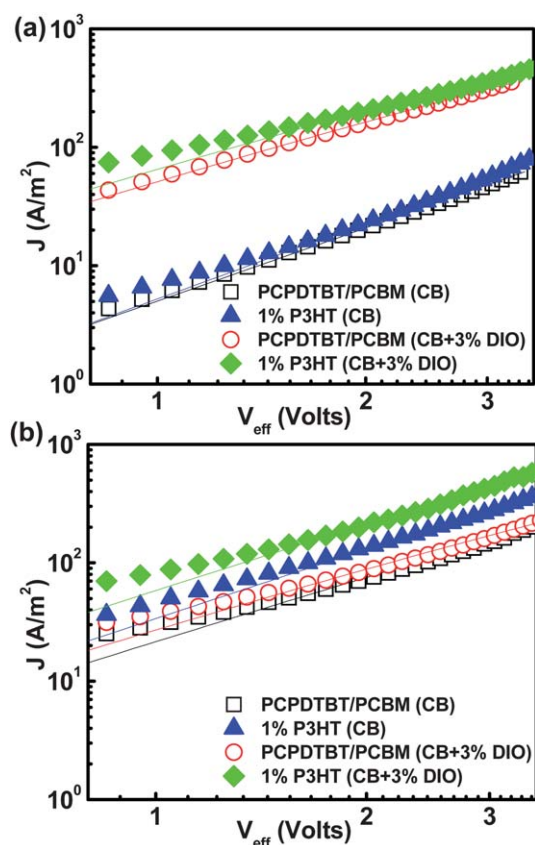


Fig. 2 The J - V characteristics and the fitting curves of (a) electron-only and (b) hole-only devices of PCPDTBT/PC61BM and PCPDTBT/PC61BM/P3HT series under dark conditions; the fitting was carried out via the space charge limited current model using a field dependent mobility.

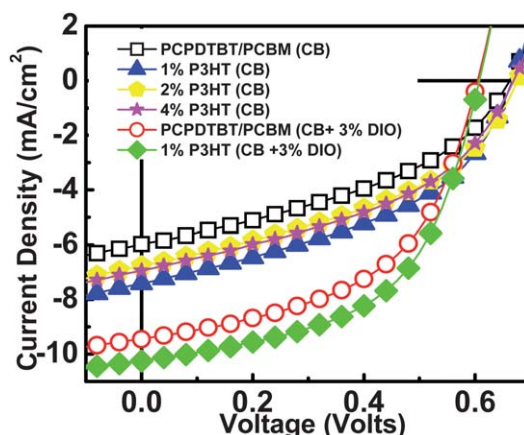


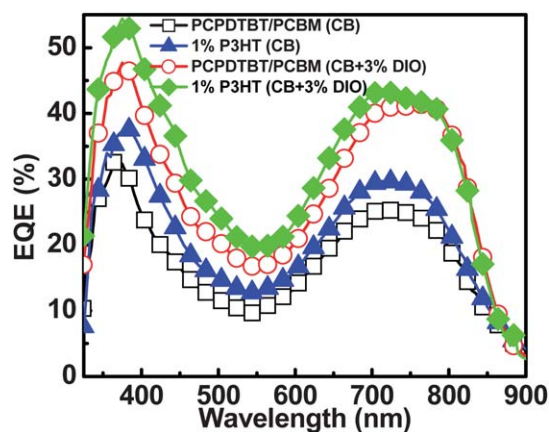
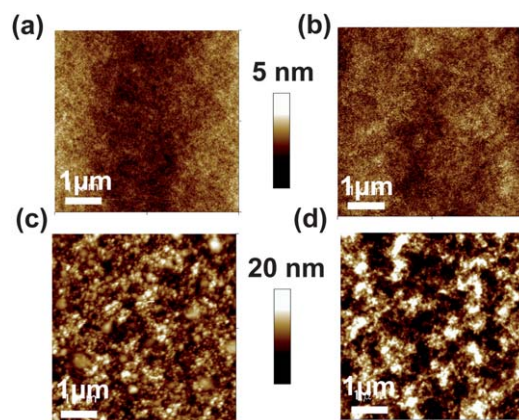
Fig. 3 The current density–voltage (J - V) curves of PCPDTBT/PC61BM (wt ratio = 10 : 36, black square), PCPDTBT/PC61BM with 1 wt% P3HT (wt ratio = 10 : 36 : 0.5, blue triangle), 2 wt% P3HT (wt ratio = 10 : 36 : 1, yellow pentagon), and 4 wt% P3HT (wt ratio = 10 : 36 : 2, purple star) processed by chlorobenzene solvent (CB); PCPDTBT/PC61BM (wt ratio = 10 : 36, red circle) and PCPDTBT/PC61BM with 1 wt% P3HT (wt ratio = 10 : 36 : 0.5, green diamond) processed by a mixed solvent of chlorobenzene and DIO (CB + 3 vol% DIO).

Table 2 The device characteristics of PCPDTBT/PC61BM and PCPDTBT/PC61BM/P3HT devices

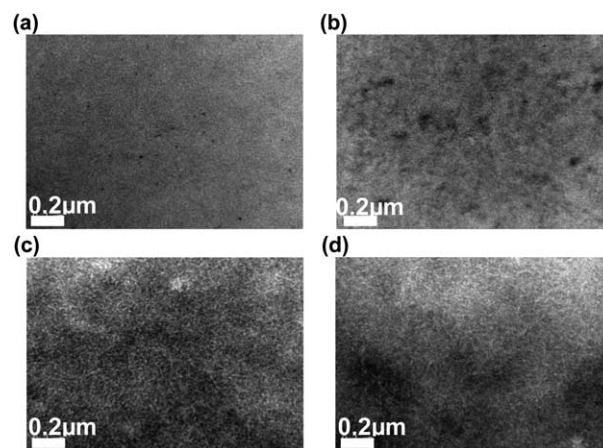
Devices	V_{oc} (V)	J_{sc} (mA cm^{-2})	FF (%)	PCE (%)
PCPDTBT/PC61BM (CB)	0.66	6.0	40.6	1.7
1% P3HT (CB)	0.67	7.4	44.2	2.2
2% P3HT (CB)	0.68	6.8	42.5	2.0
4% P3HT (CB)	0.67	6.9	42.9	2.0
PCPDTBT/PC61BM (CB + 3% DIO)	0.61	9.5	51.6	2.9
1% P3HT (CB + 3% DIO)	0.61	10.2	54.3	3.4

quantum efficiency (EQE) measurements, as shown in Fig. 4. An increase in EQE over the whole spectral range of 300–900 nm is observed, not just limited to the absorption range of 400–600 nm of P3HT. This result is quite different from other ternary cases, in which there is merely a local enhancement corresponding to the absorbance of the additive, such as PCPDTBT added into P3HT/PC61BM.^{16,34} Apparently, the P3HT acts as a morphology control agent to modulate the phase separation of either the PCPDTBT/PC61BM or PCPDTBT/PC61BM/DIO thin film, to give the desired size of crystallites and bicontinuous paths. This speculation was carefully examined in the morphology of the active layer by using AFM, TEM and GIXRD.

From the AFM scans (Fig. 5), the surface roughness of the PCPDTBT/PC61BM thin film was increased from 4.6 nm to 5.4 nm R_{rms} by the addition of 1 wt% P3HT (Fig. 5b). The noticeable change in the topography can be clearly observed due to the induced phase separation by P3HT. The addition of DIO to the processing solvent of the active layer changes the surface morphology dramatically to 19.0 nm R_{rms} , as shown in Fig. 5c. The roughness can be further increased to 26.7 nm R_{rms} by adding P3HT to the system of PCPDTBT/PC61BM/DIO (Fig. 5d). Thus, the P3HT truly acts as a morphology modulator to attain a balanced morphology between the donor and acceptor of the active layer. The morphology of the active layer was further studied by TEM. The thin film of PCPDTBT/

**Fig. 4** The EQE spectra of PCPDTBT/PC61BM (wt ratio = 10 : 36, black square), PCPDTBT/PC61BM with 1 wt% P3HT (wt ratio = 10 : 36 : 0.5, blue triangle) processed by chlorobenzene solvent (CB); PCPDTBT/PC61BM (wt ratio = 10 : 36, red circle) and PCPDTBT/PC61BM with 1 wt% P3HT (wt ratio = 10 : 36 : 0.5, green diamond) processed by a mixed solvent of chlorobenzene and DIO (CB + 3 vol% DIO).**Fig. 5** (a) 2D tapping mode AFM surface scans of films (a) PCPDTBT/PC61BM and (b) PCPDTBT/PC61BM/P3HT (1 wt%) processed by chlorobenzene solvent (CB). (c) PCPDTBT/PC61BM and (d) PCPDTBT/PC61BM/P3HT (1 wt%) processed by a mixed solvent of chlorobenzene and DIO (CB + 3 vol% DIO).

PC61BM is rather featureless, as shown in Fig. 6a. After the addition of P3HT, the domain size of the separated phase became larger and longer, as illustrated in Fig. 6b. With the addition of DIO into PCPDTBT/PC61BM, bicontinuous paths are clearly observed, as expected. Upon incorporation of P3HT into PCPDTBT/PC61BM/DIO, the size and length of the separated domains further increased for ease of charge transport, as shown in Fig. 6d. The results indicate that the aggregation of PC61BM becomes discernible from donor aggregations.^{10,29} The PC61BM clusters and the nanoscale polymer fibers constitute a complex network in the blend film. These features lead to higher phase separation of polymer and fullerene than the one without the processing additive, and further promotion of the carrier mobility in their sub-phase networks. Better transport conditions will avoid the mutual attraction of charge carriers, and the uneven density of states enables charge carriers to arrive the low energy level stages more easily.³⁵

**Fig. 6** TEM photos of films (a) PCPDTBT/PCBM and (b) PCPDTBT/PCBM/P3HT (1 wt%) processed by chlorobenzene solvent (CB). (c) PCPDTBT/PCBM and (d) PCPDTBT/PCBM/P3HT (1 wt%) processed by a mixed solvent of chlorobenzene and DIO (CB + 3 vol% DIO).

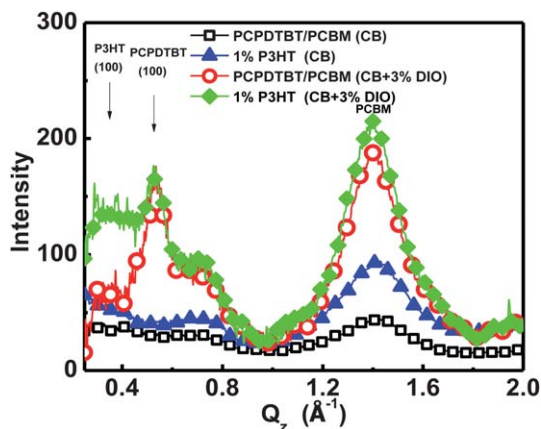


Fig. 7 Out-of-plane GIXRD profiles of the thin films of PCPDTBT/PC61BM (wt ratio = 10 : 36, black square), PCPDTBT/PC61BM with 1 wt% P3HT (wt ratio = 10 : 36 : 0.5, blue triangle) processed using chlorobenzene solvent (CB). The other sets of data are PCPDTBT/PC61BM (wt ratio = 10 : 36, red circle) and PCPDTBT/PC61BM with 1 wt% P3HT (wt ratio = 10 : 36 : 0.5, green diamond), which were processed by a mixed solvent of chlorobenzene and DIO (CB + 3 vol% DIO).

Moreover, the GIXRD profiles of the active layer can provide additional information on the influence of incorporating P3HT into PCPDTBT/PC61BM, as illustrated in Fig. 7. The (OOP)-100 direction of PCPDTBT intermolecular π - π stacking³⁶ covers the range from $q = 0.4$ to 0.8 \AA^{-1} , and the high intensity peak corresponding to PC61BM aggregation lies at $q = 1.40 \text{ \AA}^{-1}$. The (OOP)-010 peak of PCPDTBT in the active layer without additive can hardly be observed in the GIXRD scan. After the incorporation of 1 wt% P3HT, the scattering intensity is clearly increased along the whole range of q -values. The enhanced intensity suggests the increased the π - π stacking of PCPDTBT and the aggregation of PC61BM, which indicates an improvement of phase separation.²⁵ With the addition of DIO to the processing solvent of the PCPDTBT/PC61BM binary system, a discernible PCPDTBT (OOP)-100 peak appears at 0.53 \AA^{-1} , and the PC61BM peak becomes sharper. When 1 wt% P3HT was incorporated into the system of PCPDTBT/PC61BM/DIO to make the ternary active layer, a new peak appears between 0.30 and 0.40 \AA^{-1} , which corresponds to the P3HT (OOP)-100 direction. A slight increase of the PC61BM peak can be observed as well. All of these features indicate the improved phase separation, and are consistent with the results obtained from the AFM scans and the TEM morphology.

Conclusions

The incorporation of 1 wt% P3HT into the PCPDTBT/PC61BM system to make a ternary active layer can enhance the power conversion efficiency of the solar cell significantly. The P3HT functions as a morphology control agent, which can not only improve the phase separation of the active layer but also increase the light harvesting in the 400 to 500 nm range. Both the π - π stacking of PCPDTBT and the aggregation of PC61BM are increased to form extended bi-continuous domains for efficient charge transport. This strategy is also applicable for the DIO additive system, and the performance of the solar cell can be

further improved due to the increased charge mobility and fill factor. By adding a moderate amount of crystalline conducting polymer as a morphology control agent, effective phase separation and crystallization of the low bandgap polymer/fullerene system with an aligned bandgap can be induced to facilitate the charge transport. Our results should be very useful for improving the performance of other low gap polymer-based BHJ solar cells using the idea of a ternary blend for the active layer.

Acknowledgements

Financial support for this work obtained from the National Science Council of Taiwan (NSC 101-3113-E-002-010 and NSC 101-2120-M-002-003) is highly appreciated.

Notes and references

- 1 S. Haythem, L. Y. Lu, F. He, J. E. Bullock, W. Wang, B. Carsten and L. Yu, *ACS Macro Lett.*, 2012, **1**, 361.
- 2 F. Zhang, W. Mammo, L. M. Andersson, S. Admassie, M. R. Andersson and O. Inganäs, *Adv. Mater.*, 2006, **18**, 2169.
- 3 F. Wang, J. Luo, K. Yang, J. Chen, F. Huang and Y. Cao, *Macromolecules*, 2005, **38**, 2253.
- 4 N. Blouin, A. Michaud and M. Leclerc, *Adv. Mater.*, 2007, **19**, 2295.
- 5 J. Peet, J. Y. Kim, N. E. Coates, W. L. Ma, D. Moses, A. J. Heeger and G. C. Bazan, *Nat. Mater.*, 2007, **6**, 497.
- 6 P. Chen, S. H. Chan, T. C. Chao, C. Ting and B. T. Ko, *J. Am. Chem. Soc.*, 2008, **130**, 12828.
- 7 G. Li, Y. Yao, H. Yang, V. Shrotriya, G. Yang and Y. Yang, *Adv. Funct. Mater.*, 2007, **17**, 1636.
- 8 V. D. Mihailetschi, H. X. Xie, B. de Boer, L. J. A. Koster and P. W. M. Blom, *Adv. Funct. Mater.*, 2006, **16**, 699.
- 9 Y. Gu, C. Wang and T. P. Russell, *Adv. Energy Mater.*, 2012, **2**, 683.
- 10 J. K. Lee, W. L. Ma, C. J. Brabec, J. Yuen, J. S. Moon, J. Y. Kin, K. Lee, G. C. Bazan and A. J. Heeger, *J. Am. Chem. Soc.*, 2008, **130**, 3619.
- 11 R. J. Kline, M. D. McGehee and M. F. Toney, *Nat. Mater.*, 2006, **5**, 222.
- 12 K. Sivula, Z. T. Ball, N. Watanabe and J. M. J. Fréchet, *Adv. Mater.*, 2006, **18**, 206.
- 13 M. Reyes-Reyes, K. Kim, J. Dewald, R. Lopez-Sandoval, A. Avadhanula, S. Curran and D. Carroll, *Org. Lett.*, 2005, **7**, 5749.
- 14 U. Zhokhavets, T. Erb, H. Hoppe, G. Gobsch and N. S. Sariciftci, *Thin Solid Films*, 2006, **496**, 679.
- 15 N. Camaioni, G. Ridolfi, G. Casalbore-Miceli, G. Possamai and M. Maggini, *Adv. Mater.*, 2002, **14**, 1735.
- 16 M. Koppe, H. J. Egelhaaf, G. Dennler, M. C. Scharber, C. J. Brabec, P. Schilinsky and C. N. Hoth, *Adv. Funct. Mater.*, 2010, **20**, 338.
- 17 H. C. Hesse, J. Weickert, C. Hundschell, X. L. Feng, K. Müllen, B. Nickel, A. J. Mozer and L. S. Mende, *Adv. Energy Mater.*, 2011, **1**, 861.
- 18 Z. Hu, S. Tang, A. Ahlvers, S. I. Khondaker and A. J. Gesquiere, *Appl. Phys. Lett.*, 2012, **101**, 053308.

- 19 G. D. Sharma, S. P. Singh, M. S. Roy and J. A. Mikroyannidis, *Org. Electron.*, 2012, **13**, 1756.
- 20 C. Winder, G. Matt, J. C. Hummelen, R. A. J. Janssen, N. S. Sariciftci and C. J. Brabec, *Thin Solid Films*, 2002, **403–404**, 373.
- 21 Y. Kim, M. Shin, H. Kim, Y. Ha and C. S. Ha, *J. Phys. D: Appl. Phys.*, 2008, **41**, 225101.
- 22 N. Li, F. Machui, D. Waller, M. Koppe and C. J. Brabec, *Sol. Energy Mater. Sol. Cells*, 2011, **95**, 3465.
- 23 M. C. Wu, H. C. Liao, Y. Chou, C. P. Hsu, W. C. Yen, C. M. Chuang, Y. Y. Lin, C. W. Chen, Y. F. Chen and W. F. Su, *J. Phys. Chem. B*, 2010, **114**, 10277.
- 24 W. R. Wu, U. S. Jeng, C. J. Su, K. H. Wei, M. S. Su, M. Y. Chiu, C. Y. Chen, W. B. Su, C. H. Su and A. C. Su, *ACS Nano*, 2011, **5**, 6233.
- 25 H. C. Liao, C. S. Tsao, T. H. Lin, C. M. Chuang, C. Y. Chen, U. S. Jeng, C. H. Su, Y. F. Chen and W. F. Su, *J. Am. Chem. Soc.*, 2011, **133**, 13064.
- 26 D. Mühlbacher, M. Scharber, M. Morana, Z. Zhu, D. Waller, R. Gaudiana and C. Brabec, *Adv. Mater.*, 2006, **18**, 2884.
- 27 J. Kim, K. Lee, N. Coates, D. Moses, T. Nguyen, M. Dante and A. J. Heeger, *Science*, 2007, **317**, 222.
- 28 Y. Liang and L. Yu, *Acc. Chem. Res.*, 2010, **43**, 1227.
- 29 D. Nuzzo, A. Aguirre, M. Shahid, V. S. Gevaerts, S. C. J. Meskers and R. A. J. Janssen, *Adv. Mater.*, 2010, **22**, 4321.
- 30 V. Shrotriya, J. Ouyang, R. J. Tseng, G. Li and Y. Yang, *Chem. Phys. Lett.*, 2005, **411**, 138.
- 31 P. N. Murgatroyd, *J. Phys. D: Appl. Phys.*, 1970, **3**, 151–157.
- 32 M. Lenes, M. Morana, C. J. Brabec and P. W. M. Blom, *Adv. Funct. Mater.*, 2009, **19**, 1106.
- 33 H. Azimi, A. Senes, M. C. Scharber, K. Hingerl and C. J. Brabec, *Adv. Energy Mater.*, 2011, **1**, 1162.
- 34 T. Ameri, J. Min, N. Li, F. Machui, D. Baran, M. Forster, K. J. Schottler, D. Dolfen, U. Scherf and C. J. Brabec, *Adv. Energy Mater.*, 2012, **2**, 1198.
- 35 C. L. Braun, *J. Chem. Phys.*, 1984, **80**, 4157.
- 36 T. Agostinelli, T. A. M. Ferenczi, E. Pires, S. Foster, A. Maurano, C. Muller, A. Ballantyne, M. Hampton, S. Lilliu, M. C. Quiles, H. Azimi, M. Morana, D. D. C. Bradley, J. Durrant, J. E. Macdonald, N. Stingelin and J. Nelson, *J. Polym. Sci., Part B: Polym. Phys.*, 2011, **49**, 717, DOI: 10.1002/polb.22244.